Dealul Guran: evidence for Lower Palaeolithic (MIS 11) occupation of the Lower Danube loess steppe

Radu Iovita[1], Kathryn E. Fitzsimmons[2], Adrian Dobos[3], Ulrich Hambach[4], Alexandra Hilgers[5] & Anja Zander[5]

[1] MONREPOS Archaeological Research Centre and Museum for Human Behavioural Evolution, RGZM, Schloss Monrepos, D-56567, Neuwied, Germany

[2] Department of Human Evolution, Max Planck Institute for Evolutionary Anthropology, Deutscher Platz 6, Leipzig, D-04103, Germany

[3] Department of Palaeolithic Archaeology, Institute of Archaeology "Vasile Parvan" of the Romanian Academy of Sciences, 11 Henri Coanda Street, Sector 1, Bucharest 010667, Romania

[4] Chair of Geomorphology, University of Bayreuth, Universitätsstraße 30, Bayreuth, D-95440, Germany

[5] Institute for Geography, University of Cologne, Albertus-Magnus-Platz, Cologne, D-50923, Germany

This paper is published in full in *Antiquity* 86, no. 334, December 2012

Owing to a thick blanket of loess and other later geological disruptions, the earliest hominins to reach Europe are hard to find. To a handful of possible sites, our authors add a new assemblage of lithics with a clear local context and corroborated OSL dates. Ancient humans reached what is now Romania between 300 000 and 400 000 years ago.

Keywords: Europe, Romania, Lower Palaeolithic, hominin, lithics, mode 1, OSL dating

Supplement

This supplementary section provides additional information regarding the geological context of the region, and the relevant technical details relating to the luminescence dating of the site of

Dealul Guran. As discussed in the paper, the site of Dealul Guran was discovered as part of a systematic archaeological survey of the Lower Danube loess steppe region of south-eastern Romania. Since this region is for the most part blanketed by loess cover, the identification of sites relied on an understanding of the regional geology, in particular an appreciation of the evolution of the landscape (e.g. Fitzsimmons *et al*. in press) and of the varieties of limestone most likely to form caves and rockshelters, and which may provide raw material in the form of flint. In this respect the Peştera Valley was a highly suitable prospect for survey, owing to the exposure and near-surface burial of limestone formations. For this reason we include here an overview of the geology of the region and of the valley itself, since it provides context for the stratigraphy at the site, which was conducive as a workshop during the Palaeolithic period.

Determining the antiquity of the site presented multiple challenges. Both the antiquity of Dealul Guran and limited organic preservation precluded the use of radiocarbon dating, and most other dating techniques were similarly unsuitable in this environment. Luminescence dating, which determines the timing of sediment deposition contemporaneous with occupation, was the most suitable technique. However, conventional quartz OSL and coarse-grained IRSL measurements on feldspars did not produce reliable ages. This section describes the systematic approach and new protocols adopted in order to date the site.

Geological context of the loess steppe of south-eastern Romania

The site of Dealul Guran is located on the loess plateau of the Dobrogea region in south-eastern Romania. Much of the region from Hungary eastward to China—including Dobrogea—is blanketed by at least 5m of loess (Haase *et al.* 2007; and see Figure 1 in the main paper). Loess deposition in the middle and lower Danube basin of eastern Europe initiated more than a million years ago, and the last full glacial period has seen substantial increase in loess accumulation in this region (Marković *et al.* 2008). Unlike much of the northern European plain and the Alps, this region was never covered by glaciers or continental ice sheets, and nor did it experience tundra conditions. Consequently, its sedimentary sequences are potentially both long and complete. Long, continuous loess sequences, several decameters thick (e.g. Marković *et al*.

2008), are particularly well documented along the middle and lower Danube River basin (Fitzsimmons *et al.* in press). These provide some of the most comprehensive palaeoenvironmental records available on the European continent, reflecting the alternation of glacial-interglacial phases (Marković *et al.* 2008), the intensity of which can be quantified through pedological, environmental magnetic and geochemical analyses, and the timing of deposition of which can be measured using techniques such as luminescence. The loess cover, however, is not always uniform, particularly in the upper parts of valley slopes where underlying karstified limestone can be exposed at, or lie close to, the surface. Positions in the landscape such as these are therefore particularly well suited for archaeological exploration, and form the focus of this study.

The geology of the central and southern Dobrogea region, underlying the loess, is dominated by multiple limestone units of Jurassic–Tertiary age, within which many caves and rockshelters have formed. The limestone is blanketed by loess of variable thickness across hill slopes and plateaux, as well as alluvium associated with the Danube and its tributaries. Tectonic and seismic activity has affected not only river courses, but also the stability of the limestone formations. There are several karstic limestone units which are especially suitable prospects for human habitation, within which silicified sediments and flint nodules suitable for tool manufacture also occur. However, not only loess cover, but also the friability of some of these formations, reduces the exposure of prospective caves and rockshelters in the landscape. Tectonic and seismic activity in the region has led to frequent roof-falls which have helped preserve archaeology-bearing sediments associated with these features.

The Peştera Valley is typical of the geological context of the region. The village of Peştera lies at the confluence of several small creeks. The river downstream flows a further 16km north-west into the Danube. The river at Peştera has incised into both loess and the underlying Cretaceous–Tertiary marine and terrestrial sedimentary rocks. Aggradation subsequent to incision has resulted in a flat, broad valley floor downstream from Peştera.

The northern margin of Peştera village is flanked by two hills of Cretaceous–Tertiary age bedrock. South and central Dobrogea, within which the Peştera is located, corresponds to the

Moesian geological platform which forms the basement of the lower Danube basin. The uppermost units of this platform comprise alternating marine and fluvial sedimentary rocks of Cretaceous–Tertiary age. The bedrock sequence in the valley, which dominates source sediment at the archaeological site, is exposed in a disused quarry on the slope opposite Dealul Guran (known as Dealul Peşterica). The bedrock sequence exposed at Dealul Peşterica comprises six major units representing alternating marine and terrestrial environments relating to the evolution of the Tethys (Cretaceous) and retreat of the Paratethys (Tertiary) Seas (Dinu *et al.* 2005; Harzhauser & Piller 2007). The stratigraphy of Dealul Peşterica is summarised as follows, from oldest to youngest (see also Figure 2 in the main text):

1. Bedded calcareous glauconitic quartz sandstones representing a shallow marine environment (Avram *et al*. 1993; Melinte 2006), containing flint lenses which provided raw material for stone tools on the valley slopes opposite Dealul Guran. Fluvial erosion has created rockshelters, which are overlain by loess upstream of Peştera. This unit is not exposed on the south-western side of the valley at Dealul Guran.
2. Strongly weathered white kaolinitic sandstone, representing terrestrial tropical weathering and reworking of older units following marine regression (uppermost Cretaceous to lower Tertiary).
3. Weathered, unconsolidated transgressive sandy limestone (upper Tertiary) of mottled orange-green color, containing flints and gravels at the base. These flints occur close to the surface at Dealul Guran, and are the most likely raw material for stone tool manufacture at that site.
4. Green calcareous glauconitic sandy clays, originally deposited as calcareous sandstones in a shallow marine environment.
5. Orange sandy limestones.
6. Fossiliferous sandy limestone (upper Tertiary), which is more consolidated than the underlying units, and forms overhangs.

Luminescence dating

Sample preparation

Samples were prepared for luminescence dating under red light. For samples EVA1041 and EVA1042, quartz from the 90–200μm size fraction, and for EVA1088 and EVA1086, quartz from the 63–90μm size fraction (since there was no coarser material in these units), was chemically isolated. This process followed a protocol of sieving, digestion in dilute hydrochloric acid to remove carbonates, oxidation in hydrogen peroxide to remove organic components, mineral separation in lithium heterotungstate to remove heavy minerals (>2.68 $g \cdot cm^{-3}$) and feldspars (<2.62 $g \cdot cm^{-3}$), and etching in 40 per cent hydrofluoric acid for 60 minutes to remove feldspars and the outer rinds of quartz exposed to alpha radiation. However, single aliquot regenerative dose (SAR; Murray & Wintle 2000) optically stimulated luminescence (OSL) measurements of all but EVA1088 showed saturation of the quartz OSL signal (Supplementary Figure 1a; Supplementary Table 1). Therefore feldspars from the 63–90μm size fraction were isolated by density separation and measured using a standard SAR infrared stimulated luminescence (IRSL) protocol (Wallinga *et al.* 2000) for samples EVA1041, EVA1042 and EVA1087. The feldspars were also unsuitable for dating due to signal saturation. This was interpreted to mean that the coarser size fractions were derived from incompletely bleached, redeposited Tertiary-age bedrock. Consequently, the polymineral 4–11μm size fraction was targeted for dating, since this material has a greater likelihood of comprising adequately bleached aeolian loess. Polymineral fine grains from all samples were extracted after acid digestion and oxidation by sediment settling following agitation in a sonic bath.

In order to identify whether the saturated Tertiary-age material was potentially contaminating the IRSL signals of the polymineral fine grains, and in the absence of the availability of suitable alternative dating techniques, coarse-grained feldspar from samples EVA1041 and EVA1042 were milled and the 4–11μm fraction separated for measurement using the post-IR $IRSL_{225}$ protocol (Buylaert *et al.* 2009). These aliquots again yielded saturated signals. These results suggest that contamination of the polymineral fine grain aliquots with very bright, Tertiary-age grains is unlikely. Therefore the polymineral fine grain measurements are taken to represent the age of sediment deposition at the site.

Equivalent dose (D_e) measurements were undertaken using the SAR protocol on a TL-DA-20 reader as described in Bøtter-Jensen *et al*. (1999, 2000), using a U340 filter for quartz OSL measurements, and a D410 filter for feldspar and polymineral IRSL and post-IR IRSL measurements. All coarse grain (>63µm) aliquots were mounted onto the central 1mm of 10mm discs using silicone oil. Polymineral fine grains were deposited onto discs via solution with acetone, then dried prior to measurement. The polymineral fine grain fraction of samples EVA1041 and EVA1042 was measured using both standard IRSL (Auclair *et al.* 2003) and post-IR IRSL protocols (Buylaert *et al.* 2009) for comparison (Supplementary Table 1). The remaining samples were also measured using the post-IR IRSL protocol. Post-IR IRSL signals have been demonstrated to show less fading than standard IRSL signals (Thomsen *et al*. 2008) and are therefore less dependent on accurate fading corrections. A dose recovery test applying ~100 Gy was incorporated into the post-IR IRSL protocol for EVA1041 and yielded results within 10 per cent of unity. Marginally better dose recovery results were obtained for the 225ºC compared with the 290ºC measurement temperatures (using 250ºC and 320ºC preheats respectively). Consequently a 225ºC measurement temperature was used, although it is acknowledged that fading rates for the lower preheat may be higher (Thiel *et al.* 2011). The stimulation temperature of 225ºC was intentionally lower than the preheat temperature of 250ºC to avoid thermal transfer. The post-IR $IRSL_{225}$ signals were analysed using the integration parameters of Stevens *et al.* (2011). Anomalous fading in both the standard IRSL and post-IR $IRSL_{225}$ signals were corrected after Auclair *et al.* (2003). Following D_e measurement and final IR illumination at 325ºC for 100 s, the same aliquots were given a dose of ~300 Gy and ~30 Gy (to EVA1041, 1042, 1087, and EVA1088, 1086 respectively), and measured using standard IRSL and post-IR $IRSL_{225}$ SAR protocols, with varying storage times inserted immediately following irradiation and preheating. The samples yielded broadly Gaussian distributions (Supplementary Figure 1b, c), and therefore the D_e for each sample was calculated using the central age model of Galbraith *et al*. (1999), with the exception of quartz OSL measurements for EVA1088, for which the minimum age model (Galbraith *et al*. 1999) was deemed more suitable.

Dose rates

Dose rates were calculated using high resolution germanium gamma spectrometry, using the conversion factors of Adamiec and Aitken (1998) to calculate the beta component. These analyses showed evidence of potential disequilibrium in the uranium series decay chain, which was corrected for by incorporation of larger dose rate uncertainties. Moisture content for beta dose attenuation was determined by weighing the raw and oven-dried sample weights. The cosmic ray dose rate component was calculated using the formulae of Prescott and Hutton (1994).

Dating results

The final luminescence ages were calculated based on post-IR $IRSL_{225}$ measurements on polymineral fine grains, and quartz OSL on the 63-90 µm fraction for the youngest sample, EVA1088. Each sample produced reproducible results, yielding broadly Gaussian dose distributions (with the exception of the EVA1088 quartz results, as discussed earlier), recycling ratios within 10 per cent of unity, low residual doses (<1 per cent of the natural), and, with the exception of two samples, overdispersion below 12 per cent (EVA1087 and 1042 yielded overdispersion values of 20 per cent and 24 per cent respectively).

The sediments at Dealul Guran represent a mixture of redeposited, incompletely bleached material derived from Tertiary-age bedrock, and aeolian loess which is more likely to have been completely zeroed just prior to deposition. Both components contain quartz and feldspar. This mixture of sediments is highly likely to have contributed to the characteristics of the luminescence signal observed within the samples. Specifically, the coarser grained (>63µm) quartz and feldspar signals were saturated in all cases other than the youngest sample (EVA1088). The sediments from which EVA1088 were collected are typically more loess-rich in character compared with the underlying units, and therefore it is likely that this horizon was completely bleached through dominantly aeolian deposition. The composition of this sample also explains its higher dose rate, since loess typically contains greater concentrations of radioactive elements than sediments comprising higher proportions of limestone and glauconite, as is the case for the older units. Coarse grains from the older samples are more likely to have derived from redeposited colluvium, which if of Tertiary age would in any case yield a saturated signal. A comparison of D_e data and resulting luminescence age estimates using the different measurement protocols is shown in Supplementary Table 1. This table highlights the unsuitability of luminescence measurement on coarse grains from the site.

Polymineral fine grains yielded reproducible signals. In the case of the older samples (EVA1041, 1042, 1087), the D_e lies within the linear growth section of the IRSL curve, but close to the asymptote of the post-IR $IRSL_{225}$ curve (Supplementary Figure 1d). This latter characteristic of the post-IR $IRSL_{225}$ measurements suggests that fading is minimal, as observed by Thiel *et al*. (2011) and supported by fading tests on those aliquots, which produced *g*-values of <1. Consequently the post-IR $IRSL_{225}$ ages quoted in this paper remain uncorrected for fading. By comparison, *g*-values for the standard IRSL measurements applied to polymineral fine grains of samples EVA1041 and 1042 were calculated to 3.0±0.43 and 2.0±1.1 respectively. The fading-corrected age estimates of these samples still underestimate the ages based on post-IR $IRSL_{225}$ measurements. However, it should be acknowledged that the fading correction method of Auclair *et al.* (2003) is better suited to samples falling within the younger portion of the feldspar dose-response curve, and consequently older samples may still represent an underestimate. This may explain why the fading-corrected IRSL ages appear younger than the post-IR $IRSL_{225}$ estimates. Interestingly, the signal intensity of aliquots arising from the post-IR $IRSL_{225}$ measurements is comparable with that arising from $IRSL_{50}$ measurements. This contrasts with the observations of Thiel *et al*. (2011), based on loess sediments from Austria, and Thomsen *et al*. (2008), working on glaciofluvial and aeolian samples from northern Eurasia.

References

ADAMIEC, G. & M. AITKEN. 1998. Dose-rate conversion factors: update. *Ancient TL* 16: 37–50.

AUCLAIR, M., M. LAMOTHE & S. HUOT. 2003. Measurement of anomalous fading for feldspar IRSL using SAR. *Radiation Measurements* 37: 487–92.

AVRAM, E., L. SZASZ, E. ANTONESCU, A. BALTRES, M. IVA, M. MELINTE,T. NEAGU, S. RADAN & C. TOMESCU. 1993. Cretaceous terrestrial and shallow marine deposits in northern South Dobrogea (SE Rumania). *Cretaceous research* 14: 265–305.

BUYLAERT, J.P., A.S. MURRAY, K.J. THOMSEN & M. JAIN 2009. Testing the potential of an elevated temperature IRSL signal from K-feldspar. *Radiation Measurements* 44: 560–65.

BØTTER-JENSEN, L., V. MEJDAHL & A.S. MURRAY. 1999. New light on OSL. *Quaternary Science Reviews* 18: 303–309.

BØTTER-JENSEN, L., E. BULUR, G.A.T. DULLER & A.S. MURRAY. 2000. Advances in luminescence instrument systems. *Radiation Measurements* 32: 523–28.

DINU, C., H.K. WONG, D. TAMBREA & L. MATENCO. 2005. Stratigraphic and structural characteristics of the Romanian Black Sea shelf. *Tectonophysics* 410: 417–35.

FITZSIMMONS, K.E., S. MARKOVIC & U. HAMBACH. In press. Pleistocene environmental dynamics recorded in the loess of the middle and lower Danube basin. *Quaternary Science Reviews*.

GALBRAITH, R.F., R.G. ROBERTS, G.M. LASLETT, H. YOSHIDA & J.M. OLLEY. 1999. Optical dating of single and multiple grains of quartz from Jinmium rock shelter, northern Australia. Part 1: experimental design and statistical models. *Archaeometry* 41: 339–64.

HAASE, D., J. FINK, G. HAASE, R. RUSKE, M. PÉCSI, H. RICHTER, M. ALTERMANN & K.-D. JÄGER. 2007. Loess in Europe—its spatial distribution based on a European Loess Map, scale 1: 2,500,000. *Quaternary Science Reviews* 26: 1301–12.

HARZHAUSER, M. & W.E. PILLER. 2007. Benchmark data of a changing sea—Palaeogeography, Palaeobiogeography and events in the Central Paratethys during the Miocene. *Palaeogeography, Palaeoclimatology, Palaeoecology* 253: 8–31.

MARKOVIĆ, S.B., M.P. BOKHORST, J. VANDENBERGHE, W.D. MCCOY, E.A. OCHES, U. HAMBACH, T. GAUDENYI, M. JOVANOVIĆ, L. ZÖLLER, T. STEVENS & B. MACHALETT. 2008. Late Pleistocene loess-palaeosol sequences in the Vojvodina region, north Serbia. *Journal of Quaternary Science* 23: 73–84.

MELINTE, M.C. 2006. Cretaceous–Cenozoic paleobiogeography of the southern Romanian Black Sea onshore and offshore areas. *Geo-Eco-Marina* 12: 79–90.

MURRAY, A.S. & A.G. WINTLE. 2000. Luminescence dating of quartz using an improved single-aliquot regenerative-dose protocol. *Radiation Measurements* 32: 57–73.

PRESCOTT, J.R. & J.T. HUTTON. 1994. Cosmic ray contributions to dose rates for luminescence and ESR dating: large depths and long term variations. *Radiation Measurements* 23: 497–500.

STEVENS, T., S.B. MARKOVIĆ, M. ZECH, U. HAMBACH & P. SÜMEGI. 2011. Dust deposition and climate in the Carpathian basin over an independently dated last glacial-interglacial cycle. *Quaternary Science Reviews* 30: 662–81.

THIEL, C., J.-P. BUYLAERT, A. MURRAY, B. TERHORST, I. HOFER, S. TSUKAMOTO & M. FRECHEN. 2011. Luminescence dating of the Stratzing loess profile (Austria). Testing the potential of an elevated temperature post-IR IRSL protocol. *Quaternary International* 234: 23–31.

THOMSEN, K.J., A.S. MURRAY, M. JAIN & L. BØTTER-JENSEN. 2008. Laboratory fading rates of various luminescence signals from feldspar-rich sediment extracts. *Radiation Measurements* 43: 1474–86.

WALLINGA, J., A. MURRAY & A. WINTLE. 2000. The single-aliquot regenerative-dose (SAR) protocol applied to coarse-grain feldspar. *Radiation Measurements* 32: 529–33.

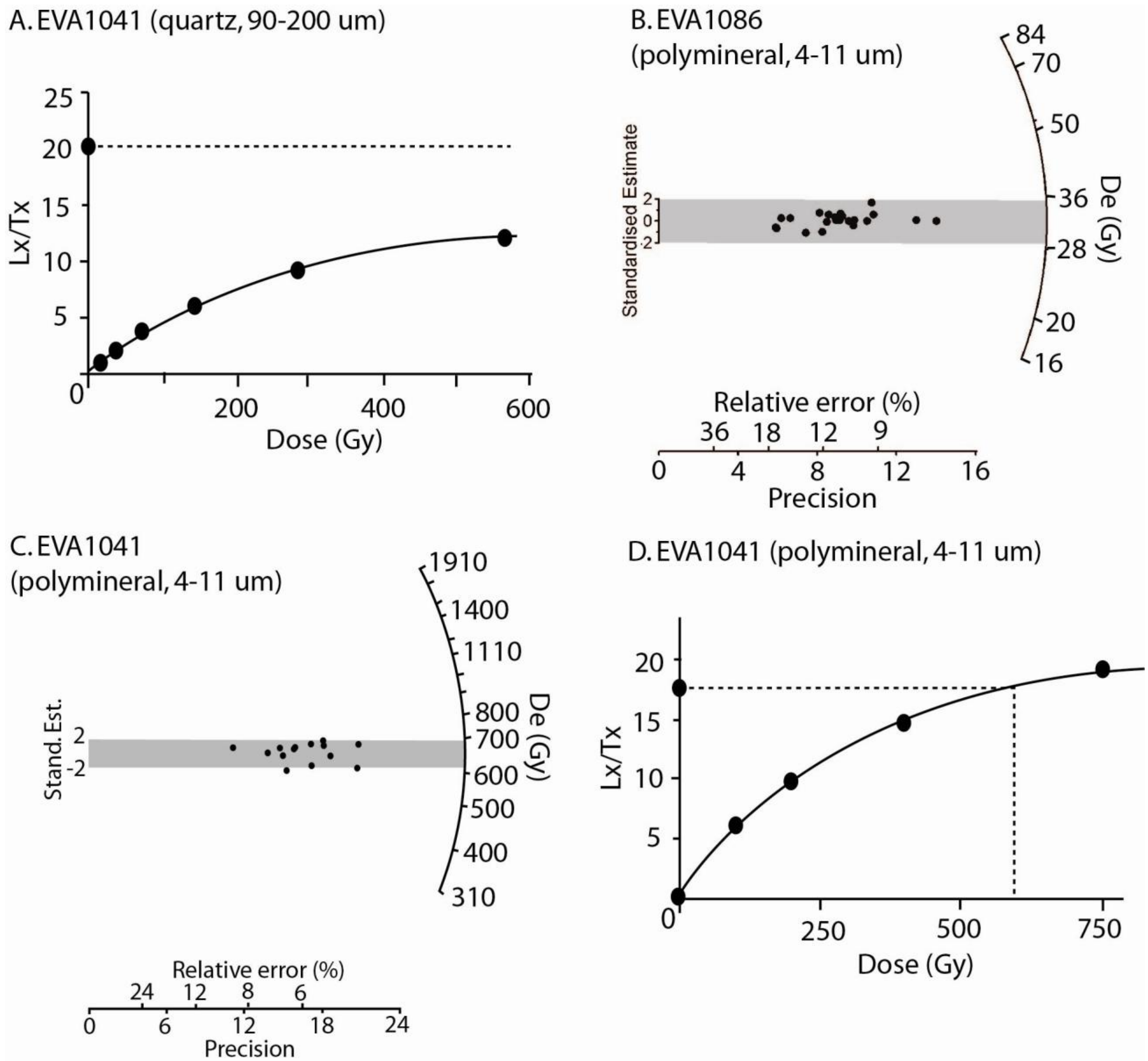

Figure 1. Luminescence data from selected samples: ***A)*** *dose-response curve for EVA1041 showing quartz OSL signal saturation for the 90–200µm size fraction;* ***B*** *and* ***C)*** *radial plots for dose distributions resulting from polymineral fine-grained post-IR IRSL measurements for EVA1086 and EVA1041, respectively. The 2σ envelope is shown by grey shading;* ***D)*** *dose-response curve, approaching saturation, for post-IR $IRSL_{225}$ measurements of 4–11µm polymineral fine grains from EVA1041, suggesting minimal fading in the post-IR $IRSL_{225}$ signal.*

Table 1. Summary of equivalent dose (D_e) data and OSL age estimates for Dealul Guran, based on measurements of different minerals using different protocols. The final accepted data for age determination are given in italics.

Sample	Mineral	Size fraction (µm)	Protocol	De (Gy)	Age (ka)
EVA1088	*Polymineral*	*4–11*	*Post-IR IRSL*	*27.4±1.4*[b]	*13.6±1.0*[b]
	Quartz	63–90	SAR	*33.5±1.0*	*17.1±1.1*
EVA1086	*Polymineral*	*4–11*	*Post-IR IRSL*	*32.5±1.0*[b]	*32.1±2.0*[b]
	Quartz	63–90	SAR	>77	>76
EVA1041	Quartz	90–200	SAR	>170	>100
	Feldspar	63–90	IRSL	>260	>153
	Feldspar	63–90	Post-IR IRSL	>243	>143
	Polymineral	4–11	IRSL	325±11[b]	252±25[c]
	Polymineral	*4–11*	*Post-IR IRSL*	*668±15*[b]	*392±23*[b]
	Milled (4-11 µm) from coarse fractions:				
	Feldspar	from 63–90	Post-IR IRSL	>860	>504
	Feldspar	from 90–212	Post-IR IRSL	>860	>504
EVA1042	Quartz	90–200	SAR	>170	>87
	Polymineral	4–11	IRSL	605±91[b]	401±125
	Polymineral	*4–11*	*Post-IR IRSL*	*756±66*[b]	*388±36*[b]
EVA1087	*Polymineral*	*4–11*	*Post-IR IRSL*	*689±19*[b]	*320±21*[b]

[a] Saturated samples. In all instances, the natural signals lay clearly above the dose-response curve (in the case of quartz, above the asymptote; for feldspars, well above even the linear growth section of the dose-response curve), such that the ages can be considered beyond the range of luminescence dating. The coarse fraction samples are therefore interpreted to reflect the Tertiary age of the source rocks.

[b] Uncorrected D_e or age estimate.

[c] Corrected for feldspar fading, after Huntley and Lamothe (2001). However, correction factors are most accurate for younger D_e values falling within the exponential part of the dose-response curve. Since these samples lie within the linear part of the curve, it is possible that the corrected age, which is younger than the post-IR IRSL age, is an underestimate.

Iovita, R., K.E. Fitzsimmons, A. Dobos, U. Hambach, A. Hilgers & A. Zander. 2012. Dealul Guran: evidence for Lower Palaeolithic (MIS 11) occupation of the Lower Danube loess steppe. *Antiquity* 86: http://antiquity.ac.uk/ant/086/ant0860973.htm